Wood Sci. Technol. 22:43–58 (1988)

Wood Science and Technology

Verification of Mukudai's mechano-sorptive model

J. Mukudai and S. Yata,* Kyoto, Japan

Summary. Mukudai and Yata have shown in the previous reports an interpretation of mechano-sorptive behavior that characteristic of viscoelastic behavior of wood under moisture change may be resulted from redistribution of applied stress in the cell wall because of change of friction between the S_1 and S_2 layers induced by moisture content change due to the looseness between the both layers, and have proposed a mechano-sorptive model based on the interpretation.

In this report, to find out evidence supporting the interpretation that mechano-sorptive behavior is resulted from the looseness between the S_1 and S_2 layers, surfaces of specimens fractured by increasing load during creep under moisture content change were observed with electron microscopes. And, characteristic features of mechano-sorptive creep and recovery deflection curves at 15%, 30% and 45% stress levels which were obtained by computer simulation were checked by comparison with those of the corresponding experiments.

As the results, it could be observed that fractures took place at the interface of the S_1 and S_2 layers in cells of the tension side of beams, and splits at the interface of the S_1 and S_2 layers took place here and there in the fractured surfaces. Furthermore, the characteristic features of creep and recovery deflection curves obtained by the simulations agreed well with those of the experiments.

Introduction

Mukudai and Yata (1986, 1987) have developed an interpretation of mechano-sorptive behavior that the characteristic viscoelastic behavior of wood under moisture change may result from redistribution of applied stress in the cell wall because of changes in friction between the S_1 and S_2 layers induced by moisture content change, and have proposed a mechano-sorptive model based on that interpretation. In the previous reports, creep and recovery under dry-wet moisture change cycles were simulated by computer by substituting viscoelastic constants and swelling and shrinkage strain into the mechano-sorptive model. These constants were estimated for each layer of the cell wall. Results of simulation agreed well with experimental results in the literature (Armstrong, Christensen 1961; Hearmon, Paton 1964; Gibson 1965).

* The authors are indebted to Professor Arno P. Schniewind, Forest Products Laboratory, University of California, for reviewing the manuscript

The purpose of this study was to verify the interpretation and the model in more detail as follows:

(1) To find evidence supporting the interpretation that mechano-sorptive behavior results from looseness between the S_1 and S_2 layers, surfaces of specimens fractured by increasing load during creep under moisture content change were observed with a scanning electron microscope.

(2) Results of computer simulation were checked with experimental results by comparison of characteristic features of mechano-sorptive creep and recovery deflection dependent on stress level of applied load.

Verification 1: Observation of surface of specimen fractured by increasing load at creep under moisture content change with a scanning electron microscope

Preparation of specimens

Beam specimens 26 cm in length (L), 0.9 cm in width (T) and about 0.7 cm in thickness (R) were cut from a heartwood block of *Cryptomeria japonica* D. Don (Sugi) so that top and bottom surfaces of beams would be latewood, to facilitate observation of microstructure of fractured cell walls. The block was air-dried under room conditions and had a specific gravity of 0.34. Sugi is suitable for such beam specimens, because this wood can be split easily with a knife at the boundary of the latewood of one growth ring and the earlywood of the next. The beams were subjected to bending moment only over a distance of 7 cm between load points at a span of 24 cm during creep. These specimens were conditioned to a constant moisture content of 21.7% (during 12 hrs at relative humidity of 95% and 30 °C) and were subjected to bending creep at a stress level of 27% under the same conditions for 12 min, and then were subjected to a relative humidity change to 20% at 30 °C (equilibrium moisture content 8.4%) for 80 min in an air conditioned chamber. During this relative humidity change, the stress level was increased 3% to 5% at intervals of 6 or 12 min so that the specimens would be fractured after about 30 min (average moisture content 17.8%) or 90 min (average moisture content 14.8%) from the start of the humidity change. During this period deflection was increasing rapidly with rapidly decreasing moisture content. Furthermore, some specimens were subjected to the same procedure after having been previously subjected to two dry-wet cycles consisting of drying for 12 h and wetting for 12 h. Creep deflections of these specimens increased during drying and increased slightly during wetting. Other specimens were fractured after 10 min from the start of creep at a stress level of 70% and a constant moisture content of 8.4%. To observe the effect of severe drying on the microstructure of the cell wall, cross section specimens 0.5 cm in thickness were cut from the same block mentioned above when wet and then were dried at 105 °C for 8 hrs. Surfaces of the fractured specimens and the cross section specimens were observed with a scanning electron microscope.

Results

The surface of a cross section dried severely at 105 °C is shown in Fig. 1. All beam specimens were fractured on the tension side. The surface of a specimen fractured during creep at constant moisture content of 8.4% is shown in Fig. 2. Surfaces of specimens fractured after 30 min and 90 min from the start of drying and after two dry-wet cycles were similar. These are shown in Figs. 3 and 4.

As shown in Fig. 1, the microstructure of the cell walls did not change visually by severe drying only. In the specimens fractured during creep at constant moisture

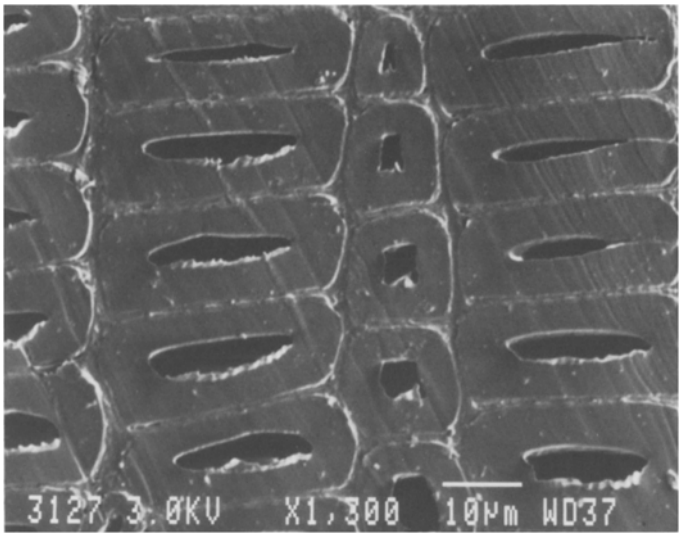

Fig. 1. Surface of cross section dried at 105 °C for 8 hrs

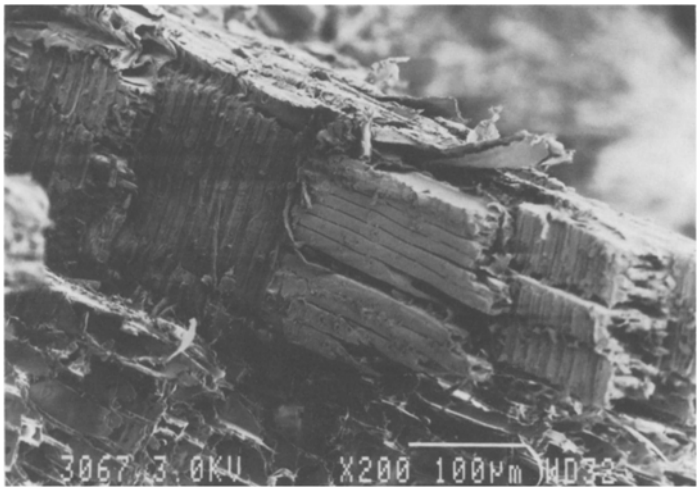

Fig. 2. Fracture of latewood on tension surface of beam failed during creep at 70% stress level and constant 8% moisture content

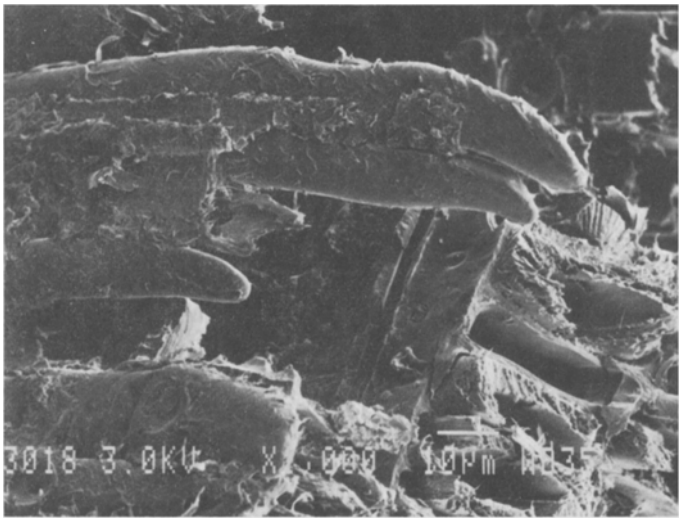

Fig. 3. Fracture of latewood on tension surface of beam failed by increasing load under drying after short-time creep at a constant moisture content of 21.7%. The tracheids with the $I+P+S_1$ layer stripped off expose surfaces of the S_2 layer, and holes from which the S_2+S_3 layer has been pulled up appear

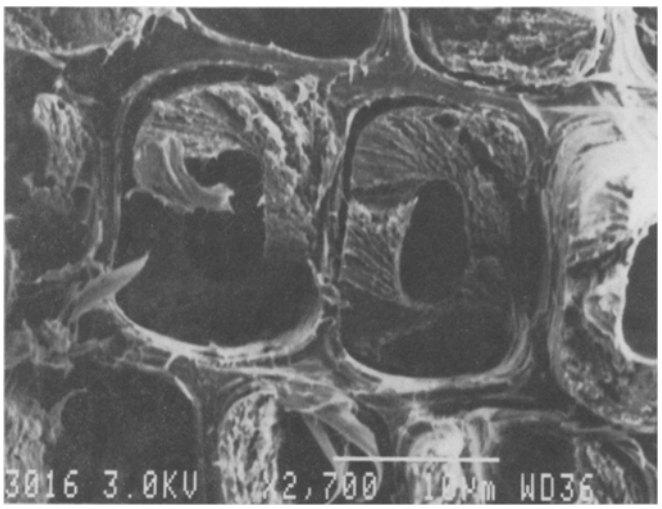

Fig. 4. Splits between the S_1 and S_2 layers in latewood cells on tension surface of beam failed by increasing load under drying after short-time creep at a constant moisture content of 21.7%

content, as shown in Fig. 2, fractured surfaces of the ray tissue were exposed here and there, and the whole fractured surface of the specimen was sliver-like. It appeared that the fracture started at a stress concentration at an interface of ray tissue and tracheids and then ran toward nearby similar interfaces. In the specimens fractured after about 30 or 90 min from the start of drying, surfaces of the S_2 layer could be observed in protruding cells that had the $I+P+S_1$ layers

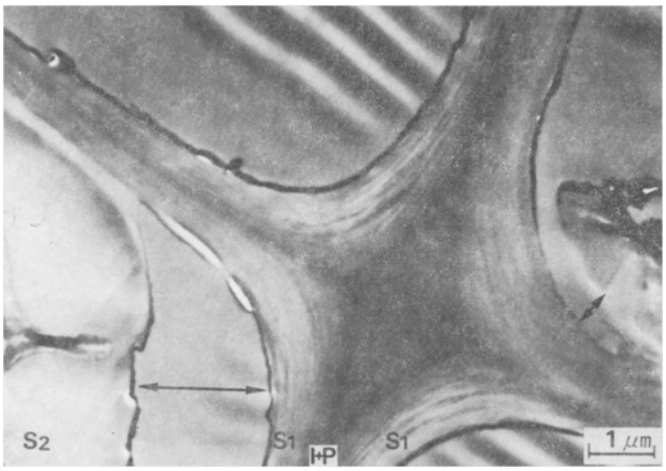

Fig. 5. Splits between the S_1 and S_2 layers observed by transmission electron microscope. Arrows in cells on the left and right show width of split. The $S_2 + S_3$ layer in cells of the upper and lower sides is out of view, far apart from the S_1 layer

stripped off, as shown in Fig. 3. Also, holes from which the S_2 layer had been pulled could be observed on the fractured surfaces. In these specimens, as shown in Fig. 4, splits at interfaces of the S_1 and S_2 layers could be observed here and there on the fractured surfaces. Fig. 5, taken by transmission electron microscope, shows more clearly that these splits were produced at interfaces of the S_1 and S_2 layers.

Verification 2: Comparison between results of experiment and simulation of creep and recovery deflection dependent on stress level

Experiment

Small specimens 11 cm in length (L), 0.47 cm in width (R) and 0.22 cm in thickness (T) were cut carefully from a sapwood block of specific gravity 0.35 of *Chamaecyparis obtusa* Endl. (Hinoki) so that they would be exactly straight-grained. These specimens were subjected to bending moment only at a distance of 6 cm between load points and a span of 10 cm. The deflection was measured at the midpoint between supports with a linear variable differential tranducer (LVDT). Stress levels of 15%, 30% and 45% of bending strength (at moisture content 11%) were used. The corresponding stresses were 90, 180 and 270 kg/cm^2, respectively. One moisture change cycle consisted of drying from 18.4% to 8.0% moisture content for 195 min and wetting from 8.0% to 18.4% for 195 min. Two schedules of creep and recovery consisting of drying and wetting were imposed as follows:

Schedule No. 1: After loading dry beams of 8.0% moisture content, creep at a constant moisture content of 8.0% for 120 min – wetting as the first step of moisture change for 195 min – drying for 195 min – six wet-dry cycles – after unloading at the end of drying of the seventh cycle, wetting recovery for 195 min – drying for 195 min – one wet-dry cycle – wetting for 600 min – five dry-wet cycles for 45% stress level only.

Stress levels used for this schedule were 15, 30 and 45%.

Schedule No. 2: After loading beams of 18.4% moisture content, creep at a constant moisture content of 18.4% for 120 min – drying as the first step of moisture change for 195 min – wetting for 195 min – five dry-wet cycles – drying for 195 min – after unloading at the end of drying of the seventh cycle, wetting recovery for 195 min – drying for 195 min – three wet-dry cycles – wetting for 300 min.

Stress levels used for this schedule were 15% and 30%, because tests at 45% stress level failed due to deflections exceeding the limited measuring range.

The tests were carried out in an air conditioned chamber changing from 30% to 95% or from 95% to 30% relative humidity at 30 °C by computer control, according to these schedules. To measure moisture content, the weight of a specimen of the same size as the bending specimens was measured with a load cell, and was checked frequently by a balance during test.

Simulation

Computer simulation was carried out using Mukudai's mechano-sorptive bending model consisting of the same sub-models of tension and compression sides as in the previous report (Mukudai and Yata 1987). Figs. 6 and 7 show the sub-model and the bending model, respectively. Viscoelastic constants of the S_2+S_3 layer were determined roughly referring to viscoelastic data of Hinoki (Mukudai 1983 a and b). Swelling and shrinkage strain of the S_2+S_3 layer was determined from published data (Barker and Meylan 1964), and that of the $I+P+S_1$ layer was regarded as twice as large as that of the S_2+S_3 layer. Unknown viscoelastic constants of the $I+P+S_1$ layer were found by trial and error, by comparing features of creep and recovery curves drawn by simulation with those from experiment. At the same time, the roughly presumed viscoelastic constants of the S_2+S_3 layer were corrected. Values of stress bias reciprocating between the S_2+S_3 layer and the $I+P+S_1$ layer due to redistribution of stress in both layers resulting from the looseness and the hoop effect due to moisture change, and the other constants were also determined. Changes of moisture content, swelling and shrinkage strain, viscoelastic constants or stress bias were given by the following equation:

$$\beta(t)=\beta_R[1-\exp(-Z\cdot t)] \tag{1}$$

where:

$\beta(t)$: Moisture content, shrinkage strain, viscoelastic constants or stress bias at time t
β_R: Range of change
Z: Constant
t: Time

The value of Z in this equation was also determined at the same time. Therefore, a great many calculations for simulation were carried out to determine the many unknown constant values.

The following was assumed according to the experimental conditions: The distance between sub-models on the tension and compression sides was 0.22 cm. The stress levels used were 15%, 30% and 45% corresponding to stresses of 90, 180

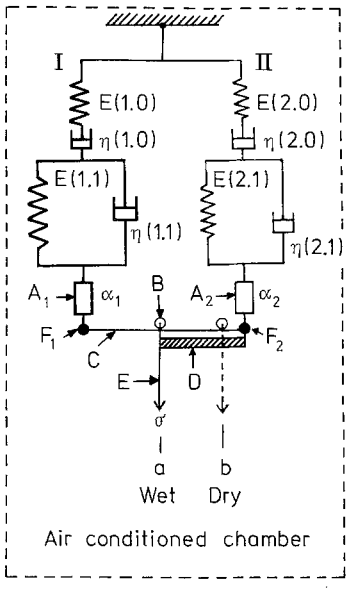

Fig. 6. Sub-model representing viscoelastic behavior of a cell of wood under moisture content change. I: S_2+S_3 layer, II: $I+P+S_1$ layer; A_1, A_2: Hygroscopic materials having swelling and shrinkage coefficient α_1, α_2, respectively; B: Running block; D: Hygroscopic material adjusting stress bias by swelling and shrinkage; F_1, F_2: Pin connection

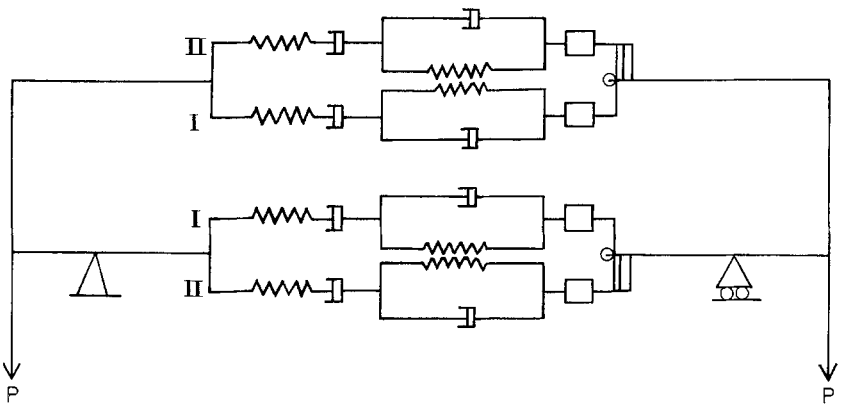

Fig. 7. Viscoelastic bending model consisting of two sub-models. I: S_2+S_3 layer, II: $I+P+S_1$ layer

and 270 kg/cm², respectively. Stresses of the appropriate level were applied to both sub-models over a distance of 6 cm between load points. The deflection was measured at the midpoint between supports. One moisture change cycle consisted of drying from 18% to 8% moisture content for 180 min and wetting from 8% to 18% for 180 min. The two imposed schedules were similar to those of the experiment. Calculation was carried out at intervals of 0.1 min. The hydrogen bond and the hoop effect were completed after 126 min from the start of a moisture change for 15% stress level, 135 min for 30% and 144 min for 45%.

Results

A set of examples of the results of experiment and simulation is shown in Figs. 8 to 17 at each stress level and for each moisture change schedule. To help clarify the simulation, a creep and recovery deflection curve at 45% stress level for schedule No. 1 is shown in Fig. 18 together with strain curves for the tension and compression sides. In each figure, deflection is shown as relative deflection (deflection as a

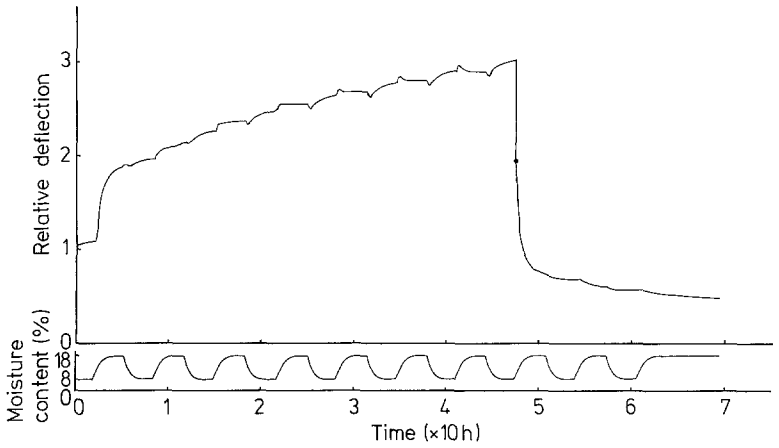

Fig. 8. Experimental creep and recovery deflection at 15% stress level (90 kg/cm²) under moisture content change cycles of Schedule No. 1. Initial deflection: 0.0738 cm; ● Deflection at elastic recovery by unloading

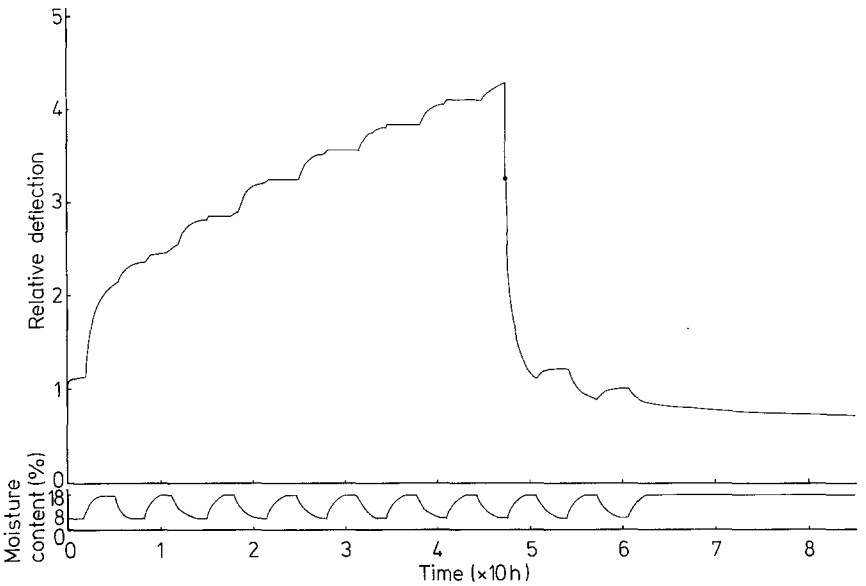

Fig. 9. Experimental creep and recovery deflection at 30% stress level (180 kg/cm²) under moisture content change cycles of Schedule No. 1. Initial deflection: 0.1068 cm; ● Deflection at elastic recovery by unloading

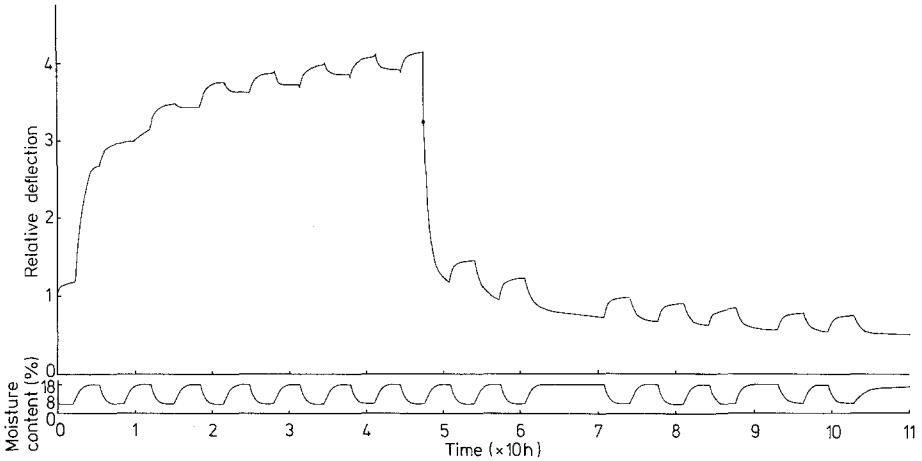

Fig. 10. Experimental creep and recovery deflection at 45% stress level (270 kg/cm²) under moisture content change cycles of Schedule No. 1. Initial deflection: 0.1870 cm; ● Deflection at elastic recovery by unloading

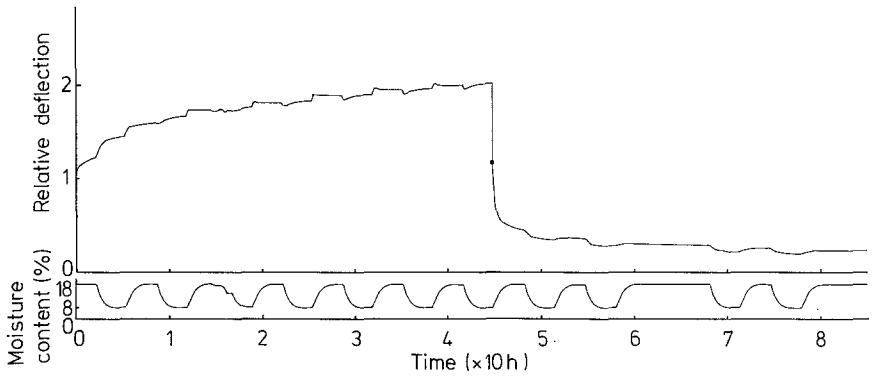

Fig. 11. Experimental creep and recovery deflection at 15% stress level (90 kg/cm²) under moisture content change cycles of Schedule No. 2. Initial deflection: 0.0640 cm; ● Deflection at elastic recovery by unloading

fraction of initial deflection at loading). Viscoelastic constants and other constants used for each simulation are shown in Table 1. The results of the experiments were as follows:

1. For both schedules, creep deflection at higher stress levels was larger.

2. In both schedules, creep deflection increased gradually with repetitions of dry-wet cycles after loading, but recovered rapidly with wetting after unloading.

3. At the first step of moisture change, creep deflection increased rapidly during wetting and drying in both schedules, and was larger under schedule No. 1 than schedule No. 2.

4. In both schedules, creep behavior after the first step was as follows:

(1) In the case of 15% stress level, a spike-like increase was produced by wetting and a similar decrease was produced by drying at the start of each moisture change.

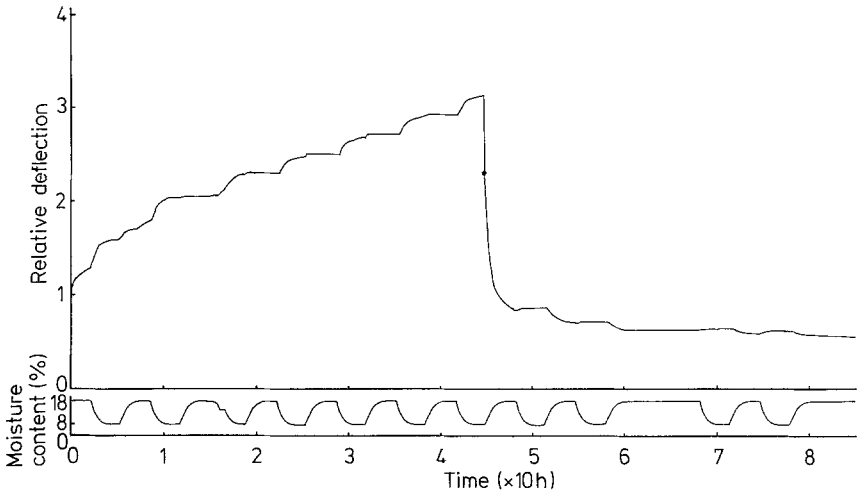

Fig. 12. Experimental creep and recovery deflection at 30% stress level (180 kg/cm²) under moisture content change cycles of Schedule No. 2. Initial deflection: 0.1195 cm; ● Deflection at elastic recovery by unloading

Table 1. Viscoelastic constants and other constants used for simulation

Layer	Viscoelastic constant[a]	15% stress level		30% stress level		45% stress level	
		Moisture content		Moisture content		Moisture content	
		8%	18%	8%	18%	8%	18%
S_2+S_3	$1/E(1,0)\times10^{-5}$ cm²/kg	1.25	1.54	1.25	1.54	1.25	1.54
	$\eta(1,0)\times10^{9}$ cm²/kg min	6.35	3.17	6.35	3.17	6.35	3.17
	$1/E(1,1)\times10^{-6}$ cm²/kg	0.80	1.60	0.80	1.60	3.00	6.00
	$\eta(1,1)\times10^{7}$ cm²/kg min	33.8	16.9	33.8	16.9	9.54	4.81
$I+P+S_1$	$1/E(2,0)\times10^{-4}$ cm²/kg	1.25	1.54	1.25	1.54	1.25	1.54
	$\eta(2,0)\times10^{9}$ cm²/kg min	5.40	2.70	5.40	2.70	5.40	2.70
	$1/E(2,1)\times10^{-4}$ cm²/kg	1.50	1.80	2.80	3.36	4.50	5.40
	$\eta(2,1)\times10^{4}$ cm²/kg min	16.9	12.0	9.00	6.43	5.68	4.10

Swelling and shrinkage strain between 8% and 18% moisture content; α_1 of S_2+S_3 layer: 0.0007, α_2 of $I+P+S_1$ layer: 0.0014

Z value in Eq. (1) for changes of moisture content, swelling and shrinkage and viscoelastic constants: 0.0333

Stress bias at 15% stress level; Stress bias for drying: 7.6 kg/cm², Stress bias for wetting: 7.3 kg/cm²

Z value in Eq. (1) for change of stress bias of 15% stress level: 0.031

Stress bias at 30% stress level; Stress bias for drying: 10.3 kg/cm², Stress bias for wetting: 9.7 kg/cm²

Z value in Eq. (1) for change of stress bias of 30% stress level: 0.195

Stress bias at 45% stress level; Stress bias for drying: 11.4 kg/cm², Stress bias for wetting: 10.6 kg/cm²

Z value in Eq. (1) for change of stress bias of 45% stress level: 0.333

[a] Reference to Fig. 6

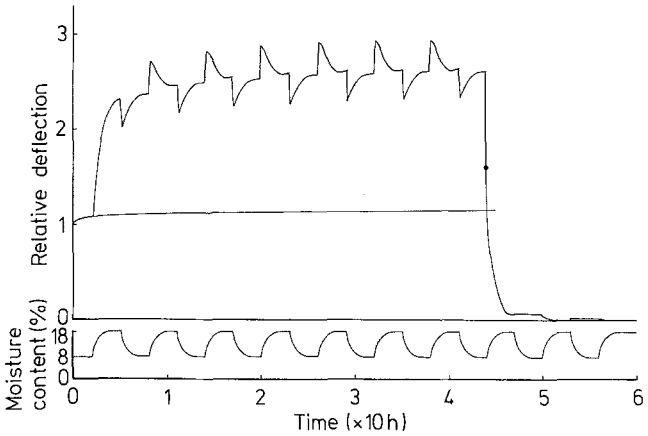

Fig. 13. Simulated creep and recovery deflection at 15% stress level (90 kg/cm²) under moisture content change cycles of Schedule No. 1. Initial deflection: 0.0418 cm; ● Deflection at elastic recovery by unloading

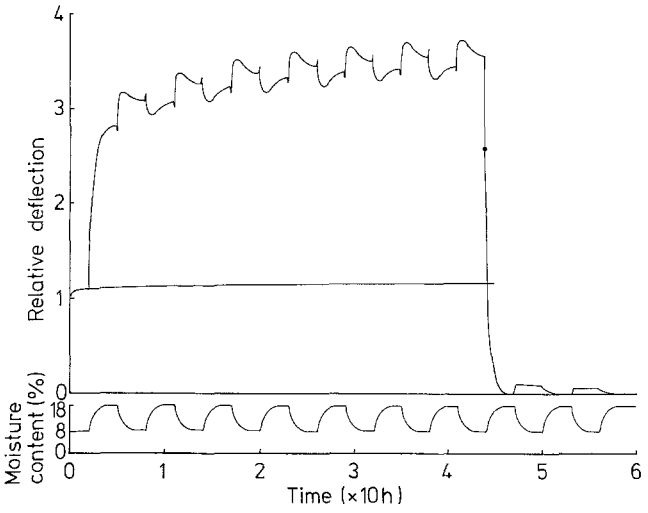

Fig. 14. Simulated creep and recovery deflection at 30% stress level (180 kg/cm²) under moisture content change cycles of Schedule No. 1. Initial deflection: 0.0836 cm; ● Deflection at elastic recovery by unloading

(2) At 30% and 45% stress levels, drying caused a large increase and wetting caused a small increase or a decrease in creep deflection.

(3) At all stress levels, an increase or a decrease in creep deflection resulting from drying or wetting was small in the first or the second cycle, but became gradually larger in succeeding cycles, and, in the case of 45% stress level, a small spike-like increase or decrease in deflection was produced at the start of wetting or drying in each of the fifth to seventh cycles.

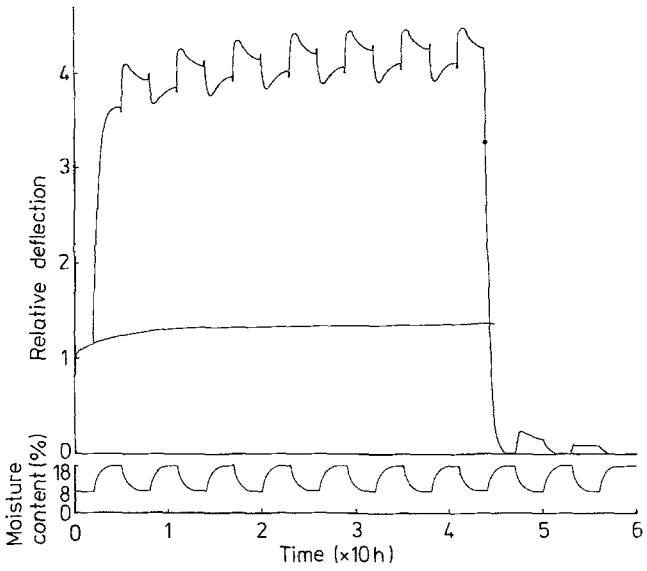

Fig. 15. Simulated creep and recovery deflection at 45% stress level (270 kg/cm²) under moisture content change cycles of Schedule No. 1. Initial deflection: 0.1255 cm; ● Deflection at elastic recovery by unloading

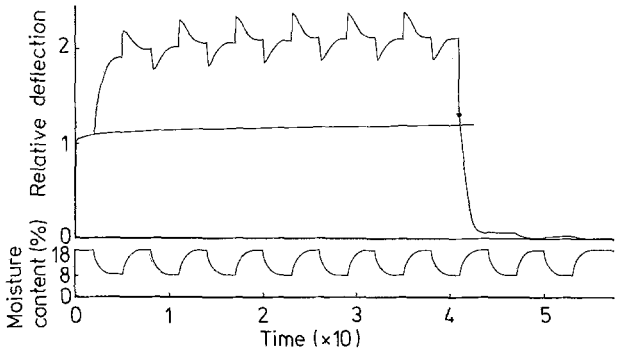

Fig. 16. Simulated creep and recovery deflection at 15% stress level (90 kg/cm²) under moisture content change cycles of Schedule No. 2. Initial deflection: 0.0516 cm; ● Deflection at elastic recovery by unloading

5. In both schedules, recovery deflection changed very little during drying but decreased during wetting at 15% stress level, and increased during drying but decreased during wetting at 30% and 45% stress levels. The increase in recovery deflection during drying decreased gradually with repeated dry-wet cycles.

The characteristic features of deflection curves at 45% stress level agreed well with those of published data (Armstrong and Christensen 1961, Gibson 1965) and those at 15% stress level agreed well with the results of shear plate tests (Hearmon and Paton 1964).

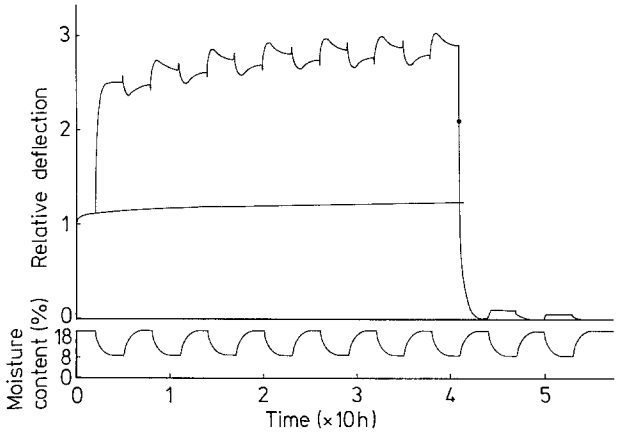

Fig. 17. Simulated creep and recovery deflection at 30% stress level (180 kg/cm²) under moisture content change cycles of Schedule No. 2. Initial deflection: 0.1032 cm; ● Deflection at elastic recovery by unloading

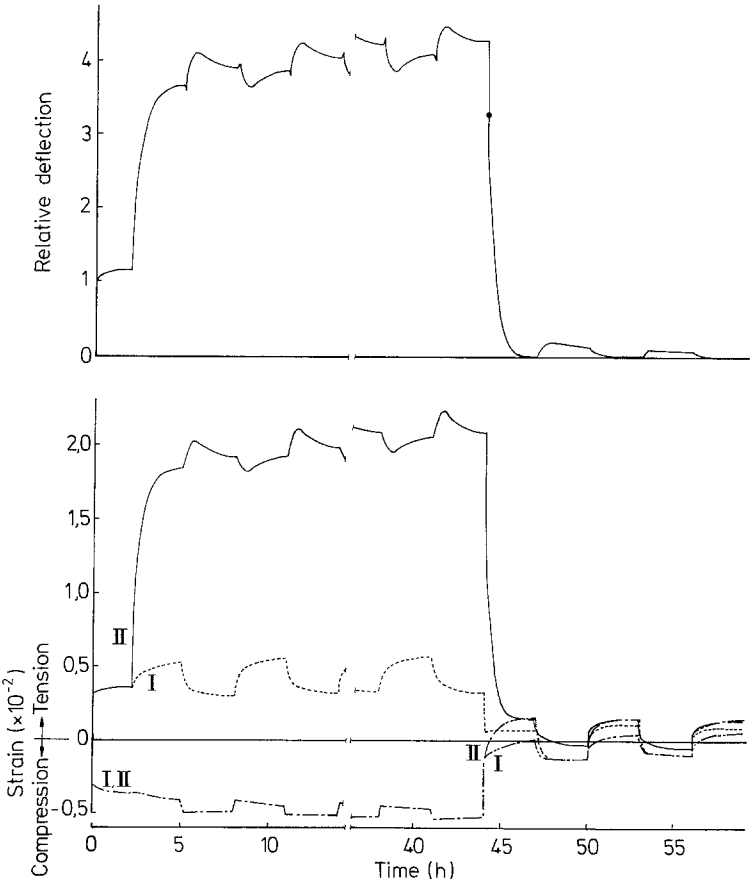

Fig. 18. Simulated creep and recovery deflection and strains of tension and compression sides at 45% stress level and Schedule No. 1. I: $S_2 + S_3$ layer, II: $I + P + S_1$ layer; Reference to Fig. 15

In this verification, the characteristic features of experimental deflection curves agreed well with corresponding curves obtained by simulation.

Discussion

Schniewind (1960) suggested that a high stress between the S_1 and S_2 layers may result from drying because of a large difference in shrinkage between the layers. Fengel (1984) showed that the interface of the S_1 and S_2 layers was split by severe drying at 150 °C for 24 hrs.

In this experiment, as mentioned in Verification 1, splitting between the S_1 and S_2 layers was not produced in specimens subjected only to drying at 105 °C, but was produced in specimens subjected to creep under moisture change. Taking account of the splitting together with such failures between the S_1 and S_2 layers as shown in Fig. 3, it is certain that the looseness between the S_1 and S_2 layers mentioned in previous reports can be produced by drying.

On the other hand, as shown in the experimental results of all stress levels in Verification 2, increases or decreases in creep deflection resulting from drying or wetting were small in the first or second cycles, and became gradually larger with repeated cycles. Characteristic features of the creep curves at each stress level appeared in the fourth to seventh cycles. The characteristic features obtained experimentally agreed well with those of simulation. The above-mentioned result suggests that there is not much looseness between the S_1 and S_2 layers during the first few cycles of moisture change, but that the looseness gradually increases with repeated cycles and that splitting between the S_1 and S_2 layers may ultimately result.

Increases of deflection in simulations were larger than observed experimentally in the first step of moisture change at all stress levels. This difference may be because restraints by the inner layer as mentioned in previous reports were not taken into account in this simulation. At all stress levels, increases or decreases in creep deflection at the start of drying or wetting were more rapid in simulations than in experiments. For example, in the case of 30% stress level, deflection at the start of drying in each cycle of simulation showed a more rapidly increasing curve than was observed in experiments. In the case of 45% stress level, increases and decreases of deflection in each cycle of simulation were also more rapid than in experiments. These differences between the results of simulation and experiment can all be interpreted as due to restraint by the inner layer.

In the case of 15% stress level, the features of the deflection curve by simulation agreed well with experimental ones because of little restraint by the inner layer. Spike-like increases and decreases at the start of moisture change were due to changes of swelling and shrinkage strain larger than those by stress bias. At this stress level, it is inferred from the simulation result that stress bias, which shifts stress from the $S_2 + S_3$ layer to the $I + P + S_1$ layer or vice versa by redistribution of stress due to moisture change, was shifted more slowly than at the higher stress levels. The z-value in Eq. (1) for stress bias was 0.031 for 15% stress level, 0.195 for 30% and 0.333 for 45%.

In the results of simulation at 30% stress level, deflection during drying increased rapidly after decreasing slightly and instantly at the start of drying, and deflection during wetting decreased rapidly after instant and slight increase at the start of wetting. On the other hand, results of experiments at this stress level showed deflection during drying increasing more than during wetting, and deflection during wetting was almost constant after instant and slight increases at the start of wetting. The differences between simulation and experiment may be due to differences in restraint by the inner layer, i.e., due to ready slippage by rapid breaking of hydrogen bonds at the start of wetting and large restraint by a slow decrease of the hoop effect at the start of drying, in the inner layer of specimens.

In the experimental results at the 45% stress level, very small spike-like increases or decreases at the start of moisture changes appeared in the fifth to seventh cycles, as shown in Fig. 10. Similar increases and decreases also appeared in all cycles of the corresponding simulation. It is inferred from the simulation that this may be attributed to ready slippage because of large increases in looseness with repeated moisture change cycles at the higher stress level.

The features of experimental recovery curves agreed well with those of simulation at all stress levels. Rapid recovery of deflection by wetting after unloading was due to release of internal stresses from breaking of hydrogen bonds between the S_1 and S_2 layers, as mentioned in the previous report. In the cases of 30% and 45% stress levels, drying during recovery induced increased deflection, the increase being larger at 45% than at 30% stress level. This increase decreased rapidly with repeated dry-wet cycles in simulation, but decreased more gradually in experiments because of restraint by the inner layer. The increase in deflection during drying did not appear at 15% stress level because of small strain at low stress and slow recovery resulting from large friction between the S_1 and S_2 layers.

As already pointed out, the characteristic features of creep and recovery deflection curves from simulation agreed well with those from experiment at each stress level, and fractures of specimens failed by increasing load after creep under drying showed evidence of supporting the authors' interpretation of mechano-sorptive behavior. It was realized from these simulations that the use of various values within a limited range of viscoelastic constants and the other constants made it possible to draw the characteristic features of mechano-sorptive creep and recovery deflection.

On the other hand, through this study, the following is inferred from the looseness and the hoop effect between the S_1 and S_2 layers: Cell walls in tree stems had swelled sufficiently and had been compressed due to supporting the upper stem and branches while in the green state during growth. Therefore, these cell walls possessed sufficient hoop effect of the S_1 layer to restrain the S_2 layer from extending laterally by swelling and compression stress. When the cell walls in wood which had been formed in such a green state are dried and are stressed in tension, looseness between the S_1 and S_2 layers may be produced naturally. Flexible bonds between the S_1 and S_2 layers in green trees presumed from the looseness in dried and tension-stressed wood, i.e., bonds depending mainly on friction resulting from the hoop effect in green trees. Such bonds give to stem and branches the flexibility necessary to resist the wind, and thus provide mechanically flexible construction.

References

Armstrong, L. D.; Christensen, G. N. 1961: Effect of moisture changes on creep in wood. Nature 191: 869–870

Barber, N. F.; Meylan, B. A. 1964: The anisotropic shrinkage of wood. Holzforschung 18: 146–156

Fengel, D.; Wegener, G. 1984: WOOD, chemistry, ultrastructure, reactions. pp. 324–325. New York: Walter de Gruyter

Gibson, E. J. 1965: Creep of wood: role of water and effect of a changing moisture content. Nature 206: 213–215

Hearmon, R. F. S.; Paton, J. M. 1964: Moisture content changes and creep of wood. Forest Prod. J. 14: 357–359

Mukudai, J. 1983 a: Evaluation on non-linear viscoelastic bending deflection of wood. Wood Sci. Technol. 17: 39–54

Mukudai, J. 1983 b: Evaluation of linear and non-linear viscoelastic bending loads of wood as a function of prescribed deflections. Wood Sci. Technol. 17: 203–216

Mukudai, J.; Yata, S. 1986: Modeling and simulation of viscoelastic behavior (tensile strain) of wood under moisture change. Wood Sci. Technol. 20: 335–348

Mukudai, J.; Yata, S. 1987: Further modeling and simulation of viscoelastic behavior (bending deflection) of wood under moisture change. Wood Sci. Technol. 21: 49–63

Schniewind, A. P. 1960: On the nature of drying stresses in wood. Holzforschung 14: 161–168

(Received February 16, 1987)

Dr. J. Mukudai
Faculty of Agriculture
Kyoto Prefectural University
Nakaragi-cho, Shimogamo
Sakyo-ku, Kyoto 606, Japan

Dr. S. Yata
Faculty of Education
Yokohama National University
Tokiwadai, Hodogaya-ku
Yokohama 240, Japan